HHS Public Access

Author manuscript

Cell Stem Cell. Author manuscript; available in PMC 2017 August 04.

Published in final edited form as:

Cell Stem Cell. 2016 August 4; 19(2): 258–265. doi:10.1016/j.stem.2016.04.014.

Zika Virus Depletes Neural Progenitors in Human Cerebral Organoids through Activation of the Innate Immune Receptor TLR3

Jason Dang[1,3], **Shashi Kant Tiwari**[1,3], **Gianluigi Lichinchi**[1], **Yue Qin**[1], **Veena S. Patil**[1], **Alexey M. Eroshkin**[2], and **Tariq M. Rana**[1,*]

[1]Department of Pediatrics and Institute for Genomic Medicine, University of California San Diego School of Medicine, 9500 Gilman Drive MC 0762, La Jolla, California, 92093, USA

[2]Bioinformatics core, Sanford-Burnham-Prebys Medical Discovery Institute, 10901 N Torrey Pines Rd, La Jolla, CA 92037 USA

Abstract

Emerging evidence from the current outbreak of Zika virus (ZIKV) indicates a strong causal link between Zika and microcephaly. To investigate how ZIKV infection leads to microcephaly, we used human embryonic stem cell-derived cerebral organoids to recapitulate early stage, first trimester fetal brain development. Here we show that a prototype strain of ZIKV MR766 efficiently infects organoids and causes a decrease in overall organoid size that correlates with the kinetics of viral copy number. The innate immune receptor Toll-Like-Receptor 3 (TLR3) was upregulated after ZIKV infection of human organoids and mouse neurospheres and TLR3 inhibition reduced the phenotypic effects of ZIKV infection. Pathway analysis of gene expression changes during TLR3 activation highlighted 41 genes also related to neuronal development, suggesting a mechanistic connection to disrupted neurogenesis. Together, therefore, our findings identify a link between ZIKV-mediated TLR3 activation, perturbed cell fate and a reduction in organoid volume reminiscent of microcephaly.

*Correspondence: trana@ucsd.edu.

[3]These authors contributed equally to this work.

ACCESSION NUMBERS

The GEO accession number for the RNA-seq data reported in this paper is GEO number GSE80264.

SUPPLEMENTAL INFORMATION

Supplemental Information includes three figures, two tables, and Supplemental Experimental Procedures and can be found with this article online at http://

AUTHOR CONTRIBUTIONS STATEMENTS

J.D. designed and performed experiments, analyzed the data, and wrote the manuscript; S.K.T. performed experiments, analyzed the data, and participated in figure preparation; G.L., performed experiments and analyzed the data; Y.Q. analyzed the data; V.S.P. performed experiments and data analysis; A. E., data analysis; T.M.R. contributed to the concept and design, data analysis and interpretation, and manuscript writing. All authors approved the final version of this manuscript.

CONFLICT OF INTEREST

The authors declare that they have no conflict of interest.

Graphical Abstract

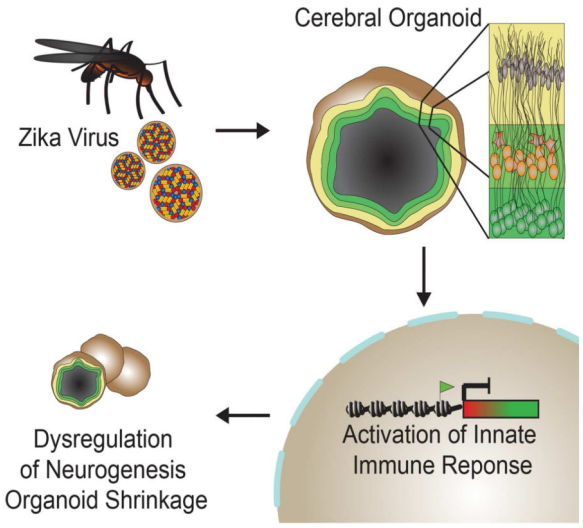

Keywords

Zika virus; microcephaly; Toll-like receptors; organoids

INTRODUCTION

Zika virus (ZIKV) of the Flaviviridae family is an emerging mosquito-borne virus originally identified in Uganda in 1947 (Driggers et al., 2016a). Outbreaks of the virus have been previously recognized in regions within Asia and Africa, including Malaysia, Thailand, Vietnam and as far as Micronesia (Driggers et al., 2016a; Hamel et al., 2015). ZIKV infects human skin and over 80% of ZIKV cases are asymptomatic or go unnoticed while the remaining cases typically exhibit mild fever, rash and joint pain for a period of 7 days (Hamel et al., 2015; Petersen et al., 2016). However, with the increased incidence due to the current outbreak of ZIKV in Brazil and throughout Latin America, new data suggests a positive correlation between cases of infection and the rise of microcephaly, characterized by abnormally small brains (Driggers et al., 2016b; Mlakar et al., 2016; Petersen et al., 2016). In fact, ZIKV was detected by electron microscopy and RT-qPCR in brains and amniotic fluid of microcephalic fetuses, strengthening the causal link between ZIKV and increased incidence of microcephaly (Calvet et al., 2016; Mlakar et al., 2016). Furthermore, recent studies show that ZIKV can infect human iPSC-derived neural progenitors in vitro, resulting in dysregulation of cell cycle related pathways and increased cell death (Tang et al., 2016). Evidence thus far suggests a strong causal relationship between ZIKV and microcephaly.

To investigate the mechanisms by which ZIKV induces microcephaly and other neurological disorders, it is essential to use scalable, reproducible in vitro models capable of recapitulating complex neurodevelopmental events during early embryogenesis. Advances in embryonic stem cell and induced pluripotent stem cell technology have opened up new avenues of disease modeling in vitro (Yamanaka, 2012). To study neurodegenerative disorders, embryonic stem cells and human derived iPSC can be differentiated towards

forebrain, midbrain and hindbrain specific neuron subtypes to model various regions of the brain. More recently, stem cells and iPSC have been differentiated into three dimensional organoid systems to study the development of the intestine, retina, liver, kidney and even the brain (Koehler and Hashino, 2014; Lancaster and Knoblich, 2014). These organoid are able to differentiate, self-organize and form distinct, complex, biologically relevant structures, thus making them ideal in vitro models of development, disease pathogenesis and drug screening. Several groups have developed cerebral organoid models that generate functional cortical neurons and can recapitulate forebrain, midbrain and hindbrain regions with functional electrophysiological properties to probe the mechanisms of neurodevelopment, autism and microcephaly (Camp et al., 2015; Eiraku et al., 2008; Lancaster et al., 2013; Mariani et al., 2015; Nowakowski et al., 2016). Previous studies have shown the use of cerebral organoid models in modeling microcephaly resulting from a heterogeneous nonsense mutation in CDK5RAP2 from patient-derived iPSC (Lancaster et al., 2013). The nonsense mutation altered the spindle orientation of radial glial cells causing a severe decrease in overall organoid size and premature differentiation of neural progenitors in the neuroepithelium. Because of the lack of outer subventricular zone (OSVZ) in mice and unknown relevance of ZIKV in mice, here we used human embryonic stem cell-derived cerebral organoids to investigate the role of ZIKV in microcephaly.

Here we show that cerebral organoids generated from human embryonic stem cells mimic the developing fetal brain and develop malformations and severely inhibited growth following ZIKV inoculation. By analyzing the transcriptomic profile of developing organoids, we draw parallels between the stunted development of ZIKV infected organoids and TLR3-mediated dysregulation of neurogenesis and axon guidance.

RESULTS

Cerebral Organoids Display Regionalization and Cortical Differentiation

To model ZIKV infection in vitro in physiologically relevant models, cerebral organoids were generated from H9 human embryonic stem cells using published protocols (Lancaster et al., 2013) with slight modifications described in the Methods section. To generate cerebral organoids, embryoid bodies were formed from embryonic stem cells using the hanging drop method and differentiated to form neuroectodermal tissue in three-dimensions (Figure 1A). Cerebral organoids display complex, self-organized internal morphology with fluid-filled ventricle-like structures similar to the developing cerebral cortex (Figure 1A and 1B). Immunohistochemistry for TUJ1 and SOX1 identify regional specificity of neuronal and neural progenitor populations, respectively (Figure 1C and S1). NESTIN positive cells exhibit elongated morphology around cavities. TUJ1 staining shows broad neuronal expression throughout the organoid tissue while SOX1 neural progenitors (NPCs) are localized in internal cavities, thereby emulating the intricate radially outward migratory pattern of differentiating neurons from the inner multiplication zone of the fetal brain.

To determine the regionalization and extent of cortical differentiation and expansion, organoids were immunostained for markers of early forebrain, hippocampus dorsal cortex and interneurons (Figure 1C). PAX6 and FOXG1 expression highlight the discrete organization of early forebrain tissue formation and specification to the ventral

telencephalon. In addition, EMX1 expression shows subregionalization of dorsal cortex regions around cavities and throughout the intermediate zone. PROX1 indicates differentiation of a portion of cerebral organoid tissue to the hippocampus while CALB2 signifies the maturation of organoid neural progenitor cells into hippocampal calretinin expressing interneurons. To confirm functional neural activity in cerebral organoids, fluctuations in cytosolic calcium content were analyzed by calcium dye imaging in response to glutamate (Figure 1D).

Cerebral Organoids Recapitulate Early Fetal Brain Development

Next, we compared the coding and non-coding transcriptome of H9 human embryonic stem cells and their derived cerebral organoids to further characterize the cerebral organoid models. 3226 and 3357 significantly differentially expressed genes with fold change >2 were identified in one month and two month old organoids when compared with undifferentiated H9 cells (Figure 2A and S2A). Gene ontology analysis of the 1642 differentially upregulated genes between organoids and embryonic stem cells show significant enrichment of genes related to neuron differentiation, development, cell morphogenesis, cell projection, axonogenesis, pattern specification and regionalization, confirming the previously shown immunostaining results (Figure 2B). On the other hand, RNA-seq analysis shows enrichment of cell cycle and mitosis related pathways in the 1584 differentially expressed downregulated genes during organoid formation, as expected. Pathway analysis of differentially expressed genes showed functionally grouped networks of developmental, neurogenesis, transcriptional, metabolic, cell cycle and cytoskeletal genes in cerebral organoid development (Figure 2C). In addition, transcriptome analysis of organoids 1 month and 2 months in culture reveal an increase in genes related to visual perception, sensory and stimulus perception, phototransduction and cognition, indicating the early formation of immature retinal tissue as cerebral organoids further develop (Figure 2D and 2E).

RNA-seq transcriptome data was then analyzed to contextualize cerebral organoids in terms of fetal brain development. Using the BrainSpan database of human brain transcriptomes, we calculated the Spearman’s correlation between in vitro differentiated cerebral organoids with post-mortem human fetal brain tissues to further assess their age and regionalization (Figure 2F, 2G and S2B) (Kang et al., 2011). Based on these analyses, organoids showed significant correlation great than 0.5 between post-mortem neocortex (temporal, parietal and occipital), ganglionic eminence (medial, lateral and caudal), cerebellum, primary motor sensory cortex, upper rhombic lip and dorsal thalamus. In addition, organoids were correlated with post-mortem fetal tissues ranging in age from 8 weeks post-conception to 21 weeks post-conception. These data indicate that the organoid tissues most resemble early trimester fetal brain tissues 8–9 weeks post-conception (Figure 2G and S2C). In all, immunohistochemistry and transcriptome analyses suggest that human embryonic stem cell-derived cerebral organoids robustly and reproducibly model early trimester fetal brains.

ZIKV Infection Abrogates Organoid Growth

To determine the effect of ZIKV on fetal brain tissue in vitro, mouse neurospheres and early day 10 human cerebral organoids were infected with the prototype MR766 ZIKV strain originating from Uganda, isolated from monkeys and expanded in Vero cells (Figure 3A).

Mouse neurospheres were utilized because of the large sample size and previous data suggesting robust reservoirs of ZIKV viral infection, ZIKV production in mouse brain tissues and the ability to recapitulate neurodegenerative phenotypes in vivo (Lazear et al., 2016; Rossi et al., 2016). ZIKV infected neurospheres exhibited significantly attenuated growth relative to control mocked treated samples (Figure 3B and 3C).

To further confirm the negative effect of ZIKV on neurodevelopment, immature day 10 human organoids were utilized for ZIKV infection because it coincides with the emergence of the neuroepithelial layer and transition from embryoid body to cerebral organoid. Cerebral organoid growth was tracked over 5 days post-infection to monitor organoid growth and development. At day 5 post-infection, healthy mock treated cerebral organoids showed an average of 22.6% increase in growth while ZIKV infected organoids significantly decreased by 16%, thus resulting in a net 45.9% difference in size on average (Figure 3D and 3F). The viral kinetics indicate a significant increase in viral copy number two days post-infection, which is reflected in the rate of change in organoid size after day 2 post-infection (Figure 3E and 3F).

To probe the effect of ZIKV in fetal brain development and in neural progenitor cells, we cryosectioned and immunostained cerebral organoids for markers of neural progenitor cells (NESTIN) and ZIKV envelope (ZIKVE) expression. We observed strong co-localization of ZIKVE in NESTIN+ cell populations compared to NESTIN− cells indicating that ZIKV infects NPCs in organoid models (Figure 3G) (Tang et al., 2016). The non-elongated cell morphology of ZIKV infected NESTIN+ cells suggests an unhealthy state and activation of apoptotic processes. Since neural progenitors and radial glial cells may be susceptible to ZIKV and infection, RT-qPCR of organoid supernatant reveals ZIKV replication and permissiveness of organoid tissues (Figure 3E). Taken together, these results demonstrate that ZIKV abrogates neurodevelopment by targeting the neural progenitor population.

ZIKV attenuates organoid growth by TLR3 activation and regulation of apoptosis and neurogenesis pathways

Previous studies have shown that ZIKV and other flaviviruses activate TLR3 in human skin fibroblasts (Hamel et al., 2015; Tsai et al., 2009). Interestingly, TLR3 has been implicated in many neuroinflammatory and neurodegenerative disorders, including in NPCs (Cameron et al., 2007; Lathia et al., 2008; Okun et al., 2010; Okun et al., 2011). TLR3 is upregulated in cerebral organoids and neurospheres after ZIKV infection as shown by RT-qPCR analysis (Figure 3E and S3C). To investigate the link between ZIKV-mediated TLR3 activation and dysregulation of neurogenesis and apoptosis, we investigated the effect of TLR3 agonist poly(I:C) and a thiophenecarboxamidopropionate compound that acts as a direct, competitive and high affinity inhibitor of TLR3 inhibitor on mouse neurospheres and human organoids. To determine the effect of TLR3 activation, neurospheres were challenged with poly(I:C) and exhibited a statistically significant decrease in overall neurosphere size relative to mock treated organoids (n>100 neurospheres per group) (Figure 4A, 4B and S3A). To further reinforce the idea that TLR3 plays a key role in ZIKV-mediated microcephaly, neurospheres were inoculated with ZIKV with TLR3 competitive inhibitor (Figure 4B and S3B). We observed a statistically significant difference between ZIKV treated neurospheres

with and without TLR3 inhibitor but no statistical significance between mock and ZIKV +inhibitor groups.

To validate our hypothesized link between ZIKV-mediated TLR3 activation and dysregulation of neurogenesis and apoptosis in an orthogonal human model, organoids were treated with TLR3 competitive inhibitor in the presences of ZIKV. Although there still appears to be cell death and disruption of the developing neuroepithelium characterized by the non-smooth outer surface of the organoid, but the TLR3 competitive inhibitor attenuated the severe ZIKV-mediated apoptosis and organoid shrinkage see in ZIKV only treated organoids (Figure 4C). These data strongly suggest that TLR3 may play a pivotal role in the ZIKV associated phenotype.

To determine the role of TLR3 activation in neurodegeneration, we compared differentially expressed genes involved in cerebral organoid formation identified by RNA-seq with differentially expressed genes following poly(I:C)-challenged TLR3 activation (data not shown) and found 41 genes in common (Figure 4D). Pathway analysis was performed to identify potential pathways by which ZIKV may regulate neurogenesis. Intriguingly, from these 41 genes, only networks relating to positive regulation of nervous system development and regulation of synapse structure or activity were significantly enriched (Figure 4D). To validate the proposed genes regulated by TLR3 that modulate neurogenesis and apoptosis in organoid development, Ntn1 and EphB2 expression levels were analyzed by RT-qPCR with ZIKV+/− inhibitor or poly(I:C) stimulation (Figure 4E, F and G). Consistent with ZIKV infection, poly(I:C) treatment of organoids reduced Ntn1 and EphB2 expression (Figure 4F). In addition, TLR3 competitive inhibitor reversed the downregulation of Ntn1 and EphB2 by ZIKV infection (Figure 4G). Altogether, these data suggest that ZIKV perturbs a TLR3 regulated network controlling neurogenesis and apoptotic pathways (Figure 4H).

DISCUSSION

Here we report the generation and application of human embryonic stem cell-derived cerebral organoids for modeling and analyzing the relationship between ZIKV and microcephaly. To properly model the complexities of the fetal brain, we employed three-dimensional organoid models capable of recapitulating regions of the developing neocortex, ganglionic eminence and retinal tissue as evidenced by immunohistochemistry and transcriptomic analyses. These in vitro cerebral organoid models present a scalable and reproducible model for neurodevelopmental and neurodegenerative studies. Organoids were then treated with prototype MR766 ZIKV to understand the phenotypic and transcriptomic response during early stage neural development. Organoids treated with ZIKV showed significant decrease in the neuroepithelium and overall organoid size.

Neurological manifestations, such as viral encephalitis, have previously been linked to other viruses of the Flaviviruses genus (Sips et al., 2012). TLR3 has been linked to neurodegenerative disorders and negative regulation of axonogenesis, as well as dengue and ZIKV infection, so we hypothesized that ZIKV activates the TLR3 pathway in neural progenitor cells, thereby leading to pro-apoptotic pathway activation and/or dysregulation of cell fate decisions (Cameron et al., 2007; Hamel et al., 2015; Okun et al., 2010; Okun et al.,

2011; Tsai et al., 2009; Yaddanapudi et al., 2011). As seen in microcephaly, dysregulated cell fate, self-renewal and apoptotic pathways in NPCs may contribute to the microcephaly phenotype. TLR3 is highly expressed in early brain development and decreases as the NPC population differentiations and the brain matures (Lathia et al., 2008). This temporally sensitive expression of TLR3 during early brain development may contribute to the trimester-specific response of fetal brains to ZIKV infection. Induction of TLR3 has been shown to trigger apoptosis by inhibiting Sonic Hedgehog and Ras-ERK signaling in NPCs and plays a role in retinopathy (Shiose et al., 2011; Yaddanapudi et al., 2011). Moreover, TLR3 has been connected to the elevated risk of neuropathological dysfunction resulting from maternal infection using TLR3-deficient mouse models (De Miranda et al., 2010). Based on these data, TLR3 likely plays a dual role that is cell type specific in which potent downstream anti-viral responses are activated in addition to tangential dysregulation of signaling networks directing apoptosis and neurogenesis.

By comparing changes in the transcriptomic profiles during cerebral organoid formation and after TLR3 activation by poly(I:C), we identified several candidate genes (Ntn1, Epha3, Adgrb3, Ephb2, Slitrk5, Syt11 and Grik2) that may be responsible for depletion of the neural progenitor population and the subsequent microcephaly phenotype through pathway analysis. Many of these TLR3 activated genes have been implicated in early brain cell fate decisions. Netrin1 is a secreted protein that works in conjunction with its dependence receptor DCC (Deleted in Colorectal Carcinoma) to regulate various pathways involved in axon guidance, apoptosis, neural cell death and cellular reprogramming (Bin et al., 2015; Furne et al., 2008; Ozmadenci et al., 2015). The role of NTN1 has been shown in vivo in floxed and null NTN1 mice. Complete loss of the gene results in severe axon guidance defects and death shortly after birth (Bin et al., 2015). Evidence suggests that NTN1 interacts with DCC to limit apoptosis but additional data has shown that the absence of NTN1 can also upregulate DCC, thus additionally triggering a pro-apoptotic cascade (Bin et al., 2015). In addition to Netrin1, the membrane-bound receptor tyrosine kinase EphB2 has been shown to be integral to fetal brain development by regulating angiogenesis, vasculogenesis and neurogenesis. EphB2 modulates radial migration, proliferation and cell fate of neural progenitor cell in the subventricular zone (Chumley et al., 2007; Katakowski et al., 2005). Interestingly, Netrin-1 and EphB2 have been shown to work synergistically through the Src family kinase-signaling pathway during neural circuit assembly (Poliak et al., 2015). However, further mechanistic studies will be required to validate the significance and underlying molecular mechanisms by which these putative genes potentially cause viral-mediated microcephaly. Nonetheless, our results present evidence that TLR3 activation of multiple genetic hubs regulating axonogenesis, cell proliferation and anti-apoptotic pathways within NPCs may strongly contribute to the ZIKV mediated microcephaly phenotype using robustly reproducible and scalable human cerebral organoid models.

Experimental Procedures

Cerebral organoid differentiation

H9 human embryonic stem cell (hESCs) (WA09) from WiCell was cultured on a feeder layer of irradiated mouse embryonic fibroblasts following previously established protocols.

All studies were conducted in accordance with approved IRB protocols by the University of California, San Diego. All animal work was approved by the Institutional Review Board at the University of California, San Diego and was performed in accordance with Institutional Animal Care and Use Committee guidelines. H9 hESCs were detached from their feeder layer using 1mg/ml collagenase for 15–20 minutes and 0.5mg/ml dispase for an additional 15 minutes. Wells were washed with media to collect floating undifferentiated hESCs and colonies were dissociated using Accumax at 37°C for 10 minutes to generate a single cell suspension. At day 0, embryoid bodies were formed using the hanging drop method with 4500 cells/drop in DMEM/F12 media supplemented with 20% knockout serum replacement, 4ng/ml bFGF, NEAA and glutamine. After 2 days of hanging drop culture, embryoid bodies were transferred to sterile petri dishes with refreshed media. After 6 days in culture, embryoid bodies were transferred to new petri dishes containing neural induction media consisting of DMEM/F12, 1:100 N2 supplement, NEAA, glutamine and 1ug/ml heparin until day 11. At day 11, organoids were transferred to Matrigel droplets and cultured in 1:1 mixture of DMEM/F12 and Neurobasal medium supplemented with 1:100 B27 without vitamin A, 1:200 N2, NEAA, insulin, beta-mercaptoethanol and glutamine. Organoids were then transferred to stir flask bioreactors for long term growth on day 15 in the same differentiation media except with the addition of retinoic acid and vitamin A. Media was changed every 3 days.

ZIKV expansion and infection

To expand prototype MR766 virus, Vero cells were inoculated with virus at MOI of 1 in E-MEM 10% FBS medium. Media was changed 24 hours after inoculation and viral supernatant was collected at 48 hours post-inoculation. Viral titer was assessed using iScript One Step RT-PCR kit (Bio-Rad) and viral copy number was calculated based on a standard curve of in vitro transcribe viral transcripts. Organoids were inoculated with ZIKV at MOI of 1.

Supplementary Material

Refer to Web version on PubMed Central for supplementary material.

Acknowledgments

We thank Steve Head and the staff of the Next Generation Sequencing core facility at The Scripps Research Institute for help with the HT-seq and data analysis, and members of the Rana lab for helpful discussions and advice. This work was supported in part by grants from the National Institutes of Health.

References

Bin JM, Han D, Lai Wing Sun K, Croteau LP, Dumontier E, Cloutier JF, Kania A, Kennedy TE. Complete Loss of Netrin-1 Results in Embryonic Lethality and Severe Axon Guidance Defects without Increased Neural Cell Death. Cell Rep. 2015; 12:1099–1106. [PubMed: 26257176]

Bindea G, Mlecnik B, Hackl H, Charoentong P, Tosolini M, Kirilovsky A, Fridman WH, Pages F, Trajanoski Z, Galon J. ClueGO: a Cytoscape plug-in to decipher functionally grouped gene ontology and pathway annotation networks. Bioinformatics. 2009; 25:1091–1093. [PubMed: 19237447]

Calvet G, Aguiar RS, Melo ASO, Sampaio SA, de Filippis I, Fabri A, Araujo ESM, de Sequeira PC, de Mendonça MCL, de Oliveira L, et al. Detection and sequencing of Zika virus from amniotic fluid of fetuses with microcephaly in Brazil: a case study. The Lancet Infectious Diseases. 2016

Cameron JS, Alexopoulou L, Sloane JA, DiBernardo AB, Ma Y, Kosaras B, Flavell R, Strittmatter SM, Volpe J, Sidman R, et al. Toll-like receptor 3 is a potent negative regulator of axonal growth in mammals. J Neurosci. 2007; 27:13033–13041. [PubMed: 18032677]

Camp JG, Badsha F, Florio M, Kanton S, Gerber T, Wilsch-Brauninger M, Lewitus E, Sykes A, Hevers W, Lancaster M, et al. Human cerebral organoids recapitulate gene expression programs of fetal neocortex development. Proc Natl Acad Sci U S A. 2015; 112:15672–15677. [PubMed: 26644564]

Chumley MJ, Catchpole T, Silvany RE, Kernie SG, Henkemeyer M. EphB receptors regulate stem/progenitor cell proliferation, migration, and polarity during hippocampal neurogenesis. J Neurosci. 2007; 27:13481–13490. [PubMed: 18057206]

De Miranda J, Yaddanapudi K, Hornig M, Villar G, Serge R, Lipkin WI. Induction of Toll-like receptor 3-mediated immunity during gestation inhibits cortical neurogenesis and causes behavioral disturbances. MBio. 2010; 1:10.

Driggers RW, Ho CY, Korhonen EM, Kuivanen S, Jaaskelainen AJ, Smura T, Rosenberg A, Hill DA, DeBiasi RL, Vezina G, et al. Zika Virus Infection with Prolonged Maternal Viremia and Fetal Brain Abnormalities. N Engl J Med. 2016a:10.

Driggers RW, Ho CY, Korhonen EM, Kuivanen S, Jaaskelainen AJ, Smura T, Rosenberg A, Hill DA, DeBiasi RL, Vezina G, et al. Zika Virus Infection with Prolonged Maternal Viremia and Fetal Brain Abnormalities. N Engl J Med. 2016b

Eiraku M, Watanabe K, Matsuo-Takasaki M, Kawada M, Yonemura S, Matsumura M, Wataya T, Nishiyama A, Muguruma K, Sasai Y. Self-organized formation of polarized cortical tissues from ESCs and its active manipulation by extrinsic signals. Cell Stem Cell. 2008; 3:519–532. [PubMed: 18983967]

Furne C, Rama N, Corset V, Chedotal A, Mehlen P. Netrin-1 is a survival factor during commissural neuron navigation. PNAS. 2008; 105:6.

Hamel R, Dejarnac O, Wichit S, Ekchariyawat P, Neyret A, Luplertlop N, Perera-Lecoin M, Surasombatpattana P, Talignani L, Thomas F, et al. Biology of Zika Virus Infection in Human Skin Cells. J Virol. 2015; 89:8880–8896. [PubMed: 26085147]

Huang da W, Sherman BT, Lempicki RA. Systematic and integrative analysis of large gene lists using DAVID bioinformatics resources. Nat Protoc. 2009; 4:44–57. [PubMed: 19131956]

Kang HJ, Kawasawa YI, Cheng F, Zhu Y, Xu X, Li M, Sousa AM, Pletikos M, Meyer KA, Sedmak G, et al. Spatio-temporal transcriptome of the human brain. Nature. 2011; 478:483–489. [PubMed: 22031440]

Katakowski M, Zhang Z, deCarvalho AC, Chopp M. EphB2 induces proliferation and promotes a neuronal fate in adult subventricular neural precursor cells. Neurosci Lett. 2005; 385:204–209. [PubMed: 15970380]

Koehler KR, Hashino E. 3D mouse embryonic stem cell culture for generating inner ear organoids. Nat Protoc. 2014; 9:1229–1244. [PubMed: 24784820]

Lancaster MA, Knoblich JA. Organogenesis in a dish: modeling development and disease using organoid technologies. Science. 2014; 345:1247125. [PubMed: 25035496]

Lancaster MA, Renner M, Martin CA, Wenzel D, Bicknell LS, Hurles ME, Homfray T, Penninger JM, Jackson AP, Knoblich JA. Cerebral organoids model human brain development and microcephaly. Nature. 2013; 501:373–379. [PubMed: 23995685]

Lathia JD, Okun E, Tang SC, Griffioen K, Cheng A, Mughal MR, Laryea G, Selvaraj PK, ffrench-Constant C, Magnus T, et al. Toll-like receptor 3 is a negative regulator of embryonic neural progenitor cell proliferation. J Neurosci. 2008; 28:13978–13984. [PubMed: 19091986]

Lazear HM, Govero J, Smith AM, Platt DJ, Fernandez E, Miner JJ, Diamond MS. A Mouse Model of Zika Virus Pathogenesis. Cell Host Microbe. 2016

Li H, Durbin R. Fast and accurate short read alignment with Burrows-Wheeler transform. Bioinformatics. 2009; 25:1754–1760. [PubMed: 19451168]

Mariani J, Coppola G, Zhang P, Abyzov A, Provini L, Tomasini L, Amenduni M, Szekely A, Palejev D, Wilson M, et al. FOXG1-Dependent Dysregulation of GABA/Glutamate Neuron Differentiation in Autism Spectrum Disorders. Cell. 2015; 162:375–390. [PubMed: 26186191]

Mlakar J, Korva M, Tul N, Popovic M, Poljsak-Prijatelj M, Mraz J, Kolenc M, Resman Rus K, Vesnaver Vipotnik T, Fabjan Vodusek V, et al. Zika Virus Associated with Microcephaly. N Engl J Med. 2016; 374:951–958. [PubMed: 26862926]

Nowakowski, Tomasz J.; Pollen, Alex A.; Di Lullo, E.; Sandoval-Espinosa, C.; Bershteyn, M.; Kriegstein, Arnold R. Expression Analysis Highlights AXL as a Candidate Zika Virus Entry Receptor in Neural Stem Cells. Cell Stem Cell. 2016

Okun E, Griffioen K, Barak B, Roberts NJ, Castro K, Pita MA, Cheng A, Mughal MR, Wan R, Ashery U, et al. Toll-like receptor 3 inhibits memory retention and constrains adult hippocampal neurogenesis. Proc Natl Acad Sci U S A. 2010; 107:15625–15630. [PubMed: 20713712]

Okun E, Griffioen KJ, Mattson MP. Toll-like receptor signaling in neural plasticity and disease. Trends Neurosci. 2011; 34:269–281. [PubMed: 21419501]

Ozmadenci D, Feraud O, Markossian S, Kress E, Ducarouge B, Gibert B, Ge J, Durand I, Gadot N, Plateroti M, et al. Netrin-1 regulates somatic cell reprogramming and pluripotency maintenance. Nat Commun. 2015; 6:7398. [PubMed: 26154507]

Petersen E, Wilson ME, Touch S, McCloskey B, Mwaba P, Bates M, Dar O, Mattes F, Kidd M, Ippolito G, et al. Rapid Spread of Zika Virus in The Americas - Implications for Public Health Preparedness for Mass Gatherings at the 2016 Brazil Olympic Games. Int J Infect Dis. 2016; 44:11–15. [PubMed: 26854199]

Poliak S, Morales D, Croteau LP, Krawchuk D, Palmesino E, Morton S, Cloutier JF, Charron F, Dalva MB, Ackerman SL, et al. Synergistic integration of Netrin and ephrin axon guidance signals by spinal motor neurons. Elife. 2015; 4

Rossi SL, Tesh RB, Azar SR, Muruato AE, Hanley KA, Auguste AJ, Langsjoen RM, Paessler S, Vasilakis N, Weaver SC. Characterization of a Novel Murine Model to Study Zika Virus. Am J Trop Med Hyg. 2016

Shannon P, Markiel A, Ozier O, Baliga NS, Wang JT, Ramage D, Amin N, Schwikowski B, Ideker T. Cytoscape: a software environment for integrated models of biomolecular interaction networks. Genome Res. 2003; 13:2498–2504. [PubMed: 14597658]

Shiose S, Chen Y, Okano K, Roy S, Kohno H, Tang J, Pearlman E, Maeda T, Palczewski K, Maeda A. Toll-like receptor 3 is required for development of retinopathy caused by impaired all-trans-retinal clearance in mice. J Biol Chem. 2011; 286:15543–15555. [PubMed: 21383019]

Sips GJ, Wilschut J, Smit JM. Neuroinvasive flavivirus infections. Rev Med Virol. 2012; 22:69–87. [PubMed: 22086854]

Tang H, Hammack C, Ogden SC, Wen Z, Qian X, Li Y, Yao B, Shin J, Zhang F, Lee EM, et al. Zika Virus Infects Human Cortical Neural Progenitors and Attenuates Their Growth. Cell Stem Cell. 2016

Tsai YT, Chang SY, Lee CN, Kao CL. Human TLR3 recognizes dengue virus and modulates viral replication in vitro. Cell Microbiol. 2009; 11:604–615. [PubMed: 19134117]

Yaddanapudi K, De Miranda J, Hornig M, Lipkin WI. Toll-like receptor 3 regulates neural stem cell proliferation by modulating the Sonic Hedgehog pathway. PLoS One. 2011; 6:e26766. [PubMed: 22046349]

Yamanaka S. Induced pluripotent stem cells: past, present, and future. Cell Stem Cell. 2012; 10:678–684. [PubMed: 22704507]

Highlights

- hESC-derived cerebral organoids model fetal brain development
- Zika virus infects neural progenitor cells in organoid and neurosphere models
- Zika virus activates Toll-like receptor 3 in cerebral organoids
- TLR3 triggers apoptosis and attenuates neurogenesis

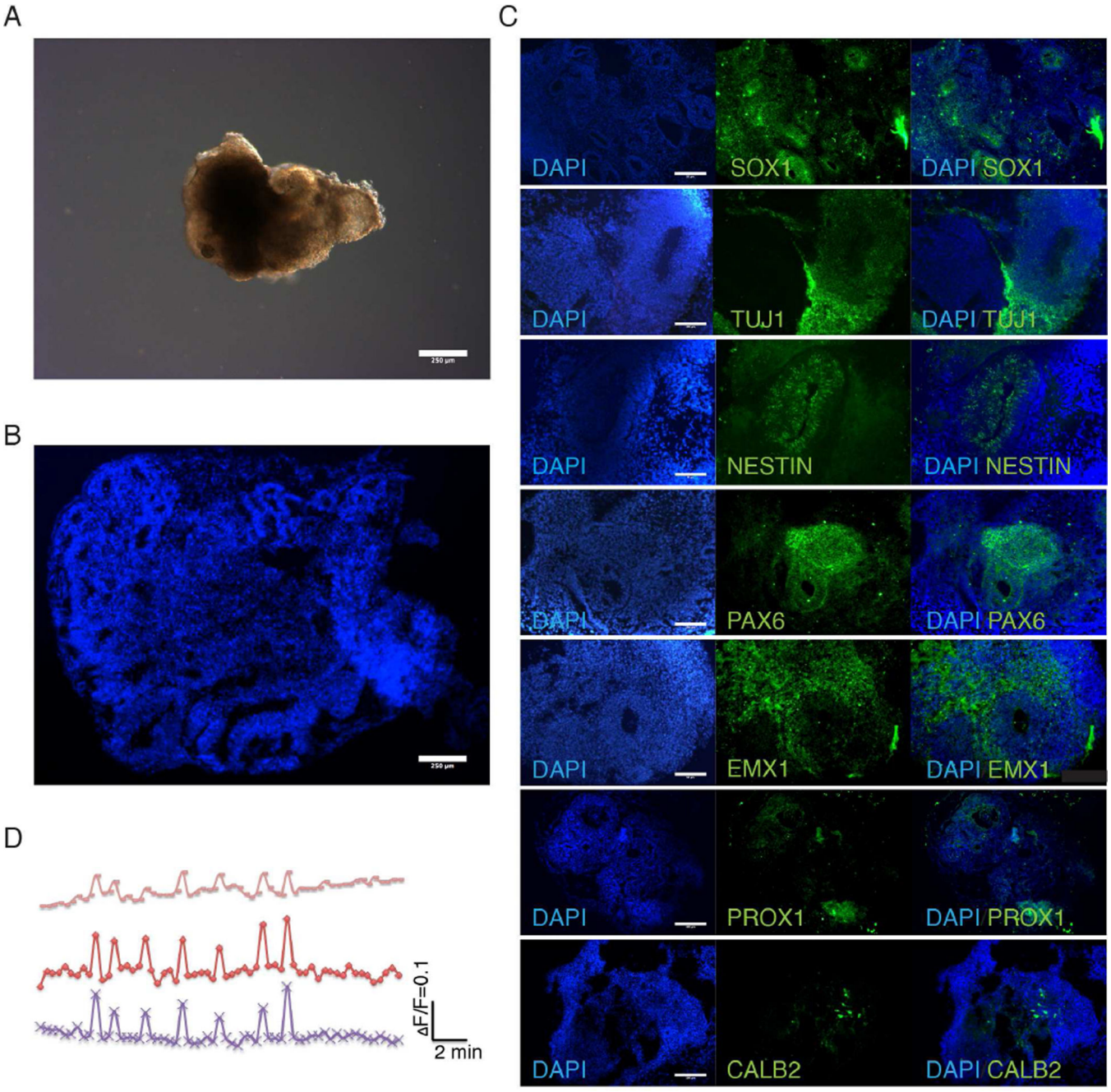

Figure 1.

Characterization of cerebral organoids reveals recapitulation of fetal brain regions. (A) Bright-field image of representative organoids show development of neuroepithelial layer. Scale bar: 250μm. (B) DAPI stained organoid shows complex inner morphology including ventricle-like structures from 30-day-old organoids. Scale bar: 250μm. (C) Organoids immunostained for neuronal (TUJ1+) and neural progenitor cells (SOX1+) cells. TUJ1 shows generalized neuronal differentiation while neural progenitors are localized near inner ventricle-like structures in 30-day-old organoids. Immunostaining for forebrain (PAX6), dorsal cortex (EMX1), hippocampus (PROX1) and interneurons (CALB2) show

differentiation of organoids into discrete brain regions 30-day-old organoids. Also see Figure S1. Scale bar: 100μm. (D) Calcium dye imaging of cerebral organoids using Fluo-4 shows functional neural activity.

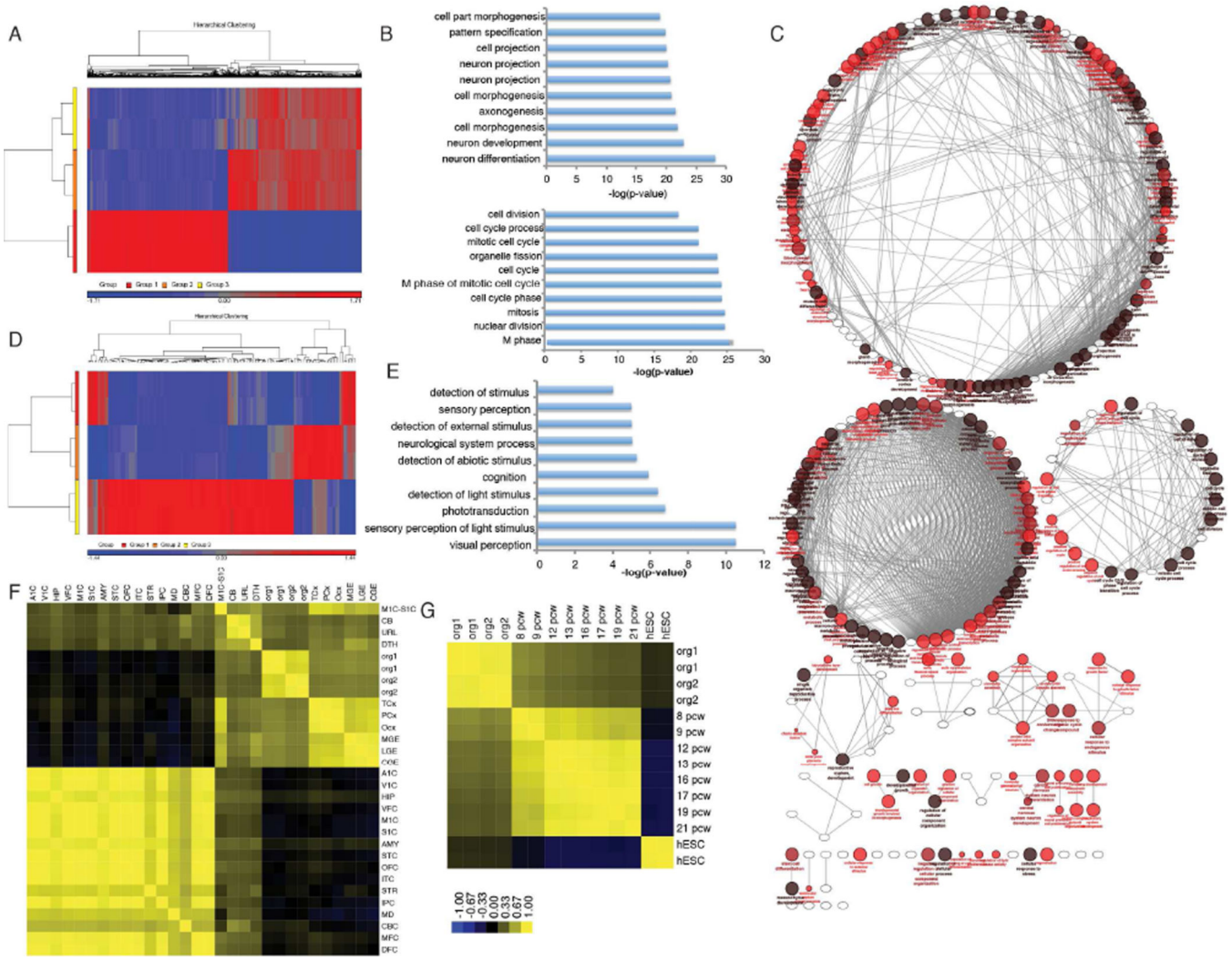

Figure 2.

RNA map of Cerebral Organoids development. (A) Heat map of transcriptome analysis from human embryonic stem cells (Group 1) and cerebral organoids after 1 month (Group 2) and 2 months (Group 3) in culture show 3226 and 3357 significantly differentially expressed genes with fold change >2, p-value <0.05. See also Figure S2A. See Table 1. (B) Gene ontology analysis show top 10 more enriched terms for upregulated (top) and downregulated (bottom) genes during cerebral organoid differentiation. (C) Grouped functional pathway analysis of differentially expressed genes during organoid formation. (D) Heat map of differentially expressed genes between organoids 1 month (Group 2) and 2 months (Group 3) in culture. Group 1 represents human embryonic stem cells. (E) Gene ontology analysis of differentially expressed genes in organoids 1 and 2 months old suggest formation of retinal tissue. (F–G) Spearman's correlation heat map of cerebral organoid transcriptomes compared with regions of the fetal brain and age post conception weeks (pcw). See Table 2 for heat map brain region legend. Also see Figure S2B and S2C.

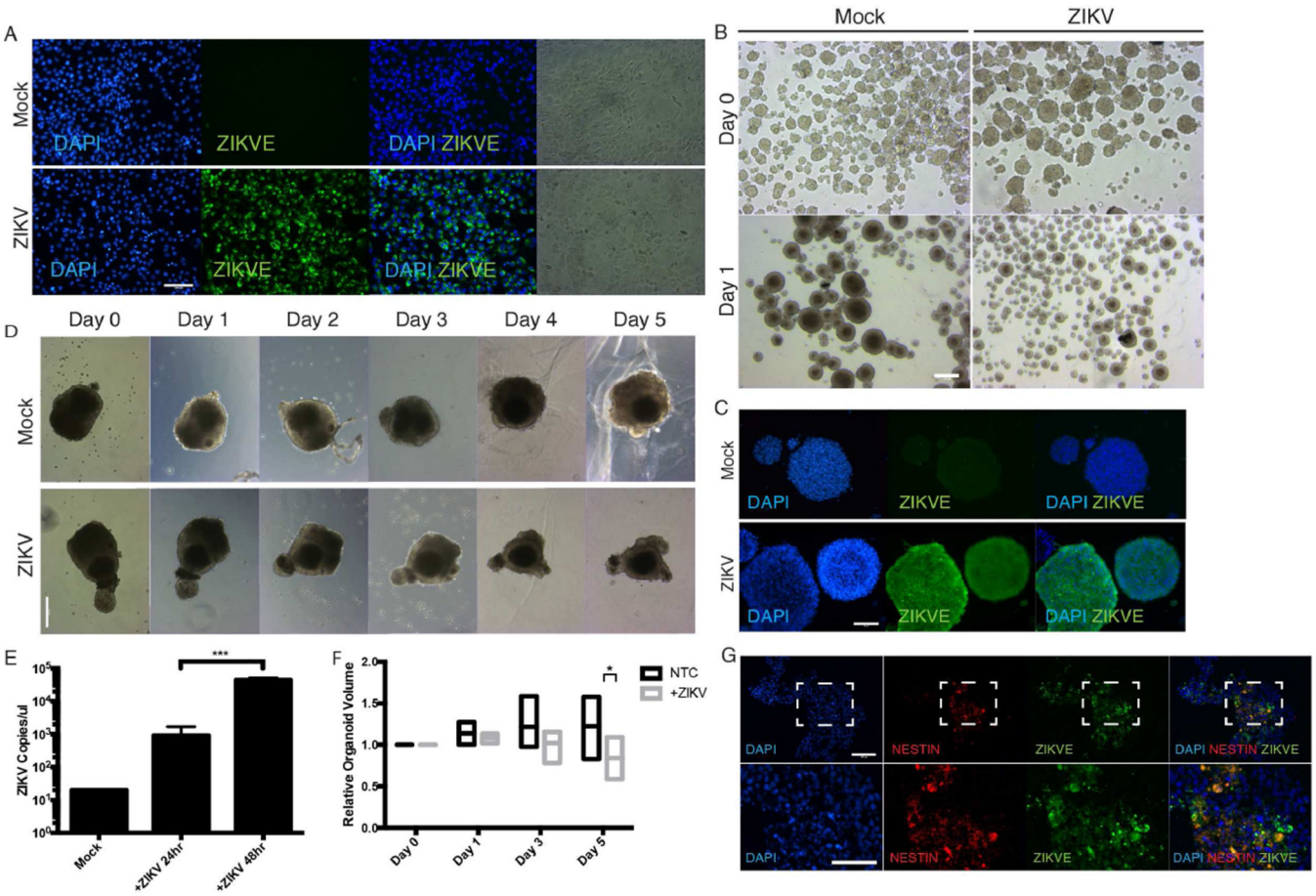

Figure 3.

ZIKV results in attenuated organoid growth in cerebral organoids and neurospheres through activation of TLR3. (A) ZIKV infected Vero cells for virus expansion. Vero cells were seeded and infected at MOI of 1 and viral supernatant was collected 48 hours post inoculation. Scale bar 100μm. (B) Bright-field images of mouse neurospheres at Day 0 and Day 1 post-inoculation with ZIKV. Scale bar: 250μm. (C) Immunohistochemistry shows ZIKV can robustly infect mouse neurospheres. Scale bar: 50μm. (D) Representative bright-field images of individual human cerebral organoids treated with ZIKV over time. Scale bar: 250μm. (E) ZIKV viral copy count in organoid supernatant quantified by one-step RT-qPCR after ZIKV infection shows organoid susceptibility and viral permissiveness. *** p-value<0.001, Student's t-test. (F) Quantification of organoid size over time with and without ZIKV infection. Bars represent the min, average and max relative organoid size. Individual organoids were measured over time relative to their respective Day 0 size from n=5 organoid samples * p-value<0.05, Student's t-test. (G) Representative images of ZIKV treated organoids stained for ZIKV envelope protein and Nestin. Scale bar: 100μm.

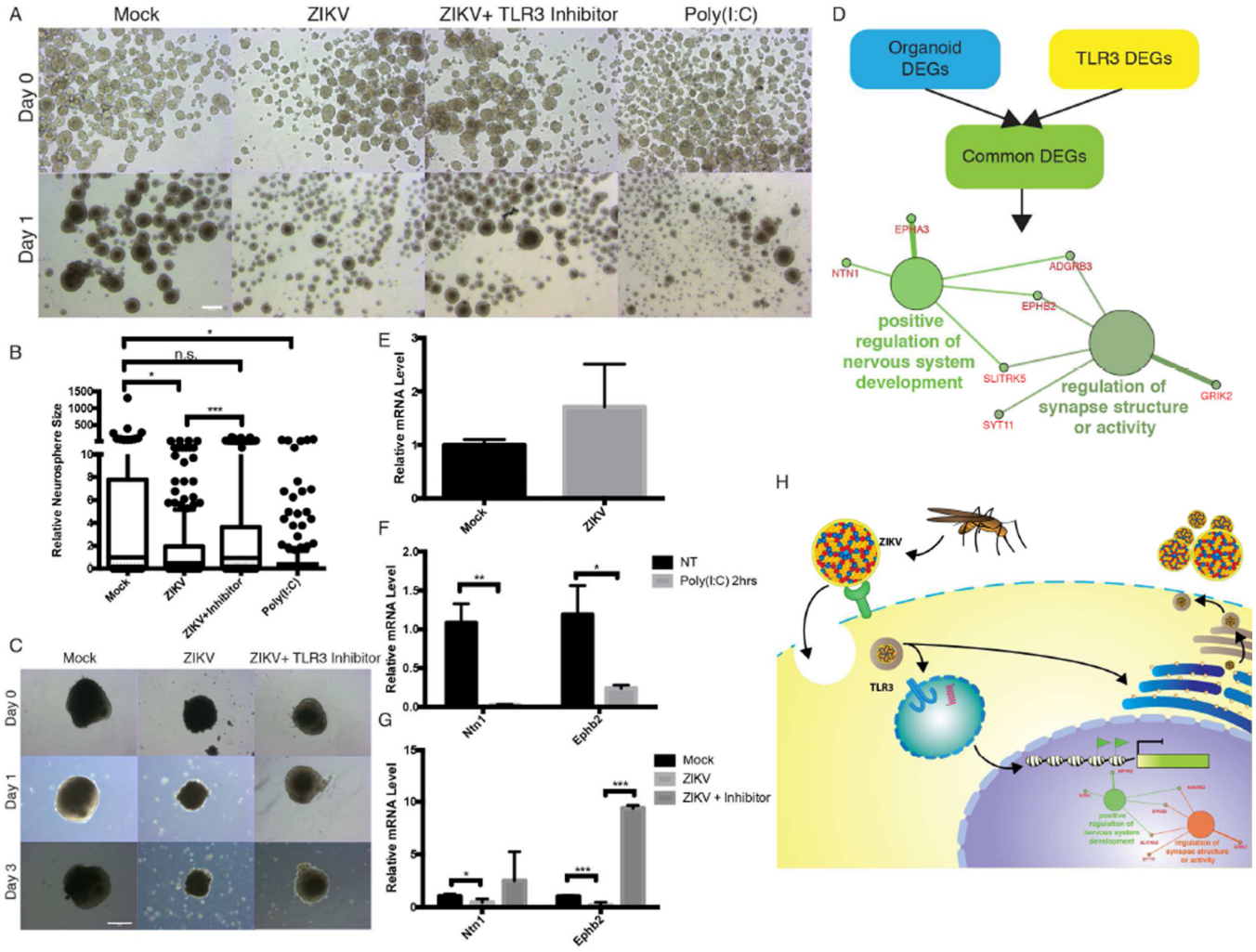

Figure 4.

ZIKV induces TLR3 and regulates pathways involved in apoptosis and neurogenesis. (A) Bright-field images of mouse neurospheres at Day 0 and Day 1 post-inoculation with ZIKV with or without TLR3 competitive inhibitor, or TLR3 agonist poly(I:C). Scale bar: 250μm. (B) Neurospheres show significant change in size 1 day post-inoculation with ZIKV with or without TLR3 competitive inhibitor, or TLR3 agonist poly(I:C) as quantified by ImageJ. Box and whiskers plot show 10–90 percentile. * p-value<0.05. *** p-value<0.001. n.s. = not significant, Student's t-test. (C) Representative bright-field images of individual human cerebral organoids treated with ZIKV with or without TLR3 competitive inhibitor. Scale bar: 250μm. (D) Schematic of target selection for RT-qPCR analyses. Differentially genes involved in organoid formation (from Figure 2A) and TLR regulated genes (data not shown) were analyzed to identify common pathways activated upon ZIKV infection. The two significantly enriched pathways from this dataset were "positive regulation of nervous system development" and "regulation of synapse structure or activity." (E) RT-qPCR analysis of TLR3 upregulation in organoids mock and ZIKV treated. Error bars represent SEM. (F) RT-qPCR analysis of differentially expressed genes, Ntn1 and EphB2, involved in TLR3 activation and neurogenesis in organoids treated with TLR3 agonist poly(I:C). Error

bars represent SEM. * p-value<0.05. ** p-value<0.01, Student's t-test. (G) RT-qPCR analysis of Ntn1 and EphB2 expression in human organoids upon ZIKV and ZIKV+ TLR3 competitive inhibitor. * p-value<0.05. *** p-value<0.001, Student's t-test. (H) Model for ZIKV infection and TLR3 mediated downregulation of regulators of neurogenesis and upregulation of pro-apoptotic pathways in NPCs.